RESEARCH ARTICLE

NA-MEMD Is Actually What You Need for Computational Pulse Analysis

HUAXING XU [1], YUNZHI TIAN[1], QIA WANG[2], XIAOBO MAO[1], YUPING ZHAO[3], AND LUQI HUANG[3]

[1]School of Electrical and Information Engineering, Zhengzhou University, Zhengzhou, Henan 450001, China
[2]Institute of Quantitative and Technological Economics, Chinese Academy of Social Sciences, Beijing 100732, China
[3]China Academy of Chinese Medical Sciences, Beijing 100020, China

Corresponding author: Qia Wang (wangqia@cass.org.cn)

ABSTRACT Time-frequency analysis is of necessity for wrist pulse signal due to its complexity, among which, empirical mode decomposition (EMD) algorithm and its improved noise-assisted versions (such as ensemble EMD, noise-assisted multivariate EMD (NA-MEMD) and very recently median EMD) are deemed to be the most representative ones. In this study, we provide an in-depth evaluation of these well-established noise-assisted EMD algorithms in computational pulse analysis for the first time. In particular, we compare the performance of the different algorithms systematically and quantitatively based on objective quantitative criteria: number and central frequency of intrinsic mode function (IMF) components, total orthogonality index and mode mixing. Rather than using synthetic signals with visual inspection in most existing literature, the wrist pulse signals used in the evaluation are real recorded samples acquired from both healthy and patient subjects. Through extensive experiments, we found that: 1) Advanced EMD algorithm that has the best performance in other areas may not be the most suitable method for pulse signal analysis, which indicates its high dependence on the type of analyzed signal; 2) Adding noise can improve algorithm performance significantly, but tends to produce physiologically irrelevant components, which however are usually neglected throughout the intelligent pulse diagnosis literature. Therefore, excluding redundant components before extracting features is expected to improve performance further. Together, currently NA-MEMD achieves a better performance consistently, potential to become a powerful tool for computational pulse analysis, but itself have not been applied in wrist pulse analysis before. We believe our works can bring up a new perspective to application of EMD-like algorithms in computational pulse analysis/diagnosis with effective information and guidance. Additionally, considering the similarity between physiological signals, especially such as photoplethysmogram/electrocardiogram, our research can be extended to wearable health monitoring technologies, including smart watches and fitness trackers, and their potential future applications, such as in heart rate estimation and evaluate various cardiovascular-related diseases. The present study underscored the necessity of evaluation noise-assisted EMDs or other adaptive decomposition algorithms based on real recorded signals with more objective measures. Especially, caution the possible redundant components that are introduced.

INDEX TERMS Computational pulse analysis, biomedical signal processing, noise-assisted EMD, objective evaluation.

The associate editor coordinating the review of this manuscript and approving it for publication was Wenbing Zhao [ID].

I. INTRODUCTION

For several thousands of years, pulse diagnosis has been one of the most popular diagnostic methods in traditional chinese medicine (TCM) community because of non-invasiveness

and convenience in health status analysis [1]. However, long-term training and high reliance on the practitioner's subjective experience limit its effectiveness in practice [2]. Over the past decade, instead of relying on subjective perception, increasing interests have been focused on developing pattern recognition techniques to perform health diagnosis in terms of measured pulse signals with advanced sensors [3], [4], [5], [6], which is referred as computational pulse analysis [7].

Basically, physiological systems are non-linear in nature and exhibit complex behaviour [8]. Controlled by the sympathetic nervous system, pulse signal exhibits variations in its characteristics, which represents non-stationary and complex properties associated with the signal, especially in abnormal health conditions [9].The classical analysis methods in signal processing (such as fast Fourier transform [10], [11] and cepstral analysis technique [12]), maybe inefficient, necessitating a more advanced time-frequency analysis. For decades, many efforts have been devoted to develop time-frequency analysis methodologies (mainly short-time fourier transform [13], [14], [15] and wavelet (packet) transform [16], [17], [18], etc.) to standardize and quantify wrist pulse analysis. Despite their success, each of these-mentioned methods still suffers from some inherent deficiencies. For example, wavelet (packet) transform is signal non-adaptive that usually require well-chosen prior kernels or basis functions [19], whereas all these methods cannot achieve arbitrary fine resolutions in both time domain and frequency domains simultaneously, restricted by the Heisenberg uncertainty principle [20].

Concurrently, on the other hand, an adaptive decomposition technique called empirical mode decomposition (EMD) algorithms [21], which overcome the limitations of the traditional time-frequency methods, has attracted considerable attention in the past decade. Since its inception, EMD has demonstrated its capabilities in many application areas, including biomedical fields related to our research, such as electroencephalogram (EEG) [22], electrocardiogram (ECG) [23]. However, unlike ECG, application of EMD algorithms to wrist pulse signals are relatively lagged behind. To our best knowledge, the earliest research can be traced back to 2006, when Sun *et al.* [24] made the first attempt to use the vanilla EMD algorithm to analyze the marginal spectrum of pulse signals of normal people and patients with coronary heart disease, demonstating potential broad prospects in pulse signal processing. Subsequently, studies have been further advanced to employ the vanilla EMD for feature extraction to better distinguish healthy subjects from patients with certain diseases, such as hypertension [25], nephritis and cholecystitis [17] and coronary heart disease [26], [27], [28].

However, the vanilla EMD method still have to face some problems, such as interpolation choice and noise sensitivity, especially prone to mode mixing, which isn't uncommon in practical recorded signals. To address these issues, a family of noise-assisted EMD methods including the ensemble EMD (EEMD) [29], the noise-assisted multivariate EMD

(NA-MEMD) [30], [31] and the very recently median EMD (MEMD) [32], have shown appealing results in various fields. For computational pulse analysis/diagnosis, one natural question arise: which of these well-established noise-assisted EMD algorithms is the most suitable, especially considering that aforementioned noise-assisted methods have not been fully explored in the TCM community.

Based on this motivation, a comprehensive and systematic understanding of vanilla EMD and three improved versions named EEMD, MEMD and NA-MEMD, for wrist pulse signal analysis, is presented in this paper. To be specific, rather than using artificial signals with visual inspection in most existing literature, we evaluate the performance of EMD algorithms on large numbers of real pulse signals, which are acquired from patient and health individuals. Moreover, multiple quantitative measures such as number and central frequency of intrinsic mode function (IMF) components, total orthogonality index and mode mixing are employed to obtain some reliable findings, guiding objectively to select the appropriate EMD algorithm for computational pulse analysis/diagnosis in TCM community.

The main contributions of this paper are summarized as follows:

1) The performance of widely-used EMD algorithms are compared systematically and quantitatively with various measures on real pulse signals. For algorithm selection in practical pulse analysis, some valuable conclusions drawn from the results are available.

2) Currently, NA-MEMD shows a remarkable performance improvement and is preferred over the others, which are suitable otherwise but not for pulse signals. However, there is still a gap with the ideal condition expected by IMF, indicating these deficiencys of vanilla EMD algorithm can be reduced but not be avoided, at least for now.

3) Redundant components introduced in noise-assisted EMD algorithms to improve performance should be devoted more attention, rather than being frequently unnoticed. This issue will likely result in serious performance degradation in classification diagnosis when some IMF features involving no real signal information but noise are used as features.

The remainder of this paper is structured as follows. Signal acquisition experiment as well as signal pre-processing are presented In Section II. Section III briefly review mathematical theory of evaluated EMD algorithms, followed by introducing four quantitative performance indicators in Section IV. Section V evaluates the performance of pulse decomposition with EMD algorithms and in terms of indicators. Results are discussed in Section VI and conclusions are drawn in Section VII.

TABLE 1. Physical characteristics of healthy and CVD groups.

	Male/Female	Age[year]	Height[cm]	Weight[kg]
Health	85/85	20.4($\pm$0.8)	171.8($\pm$7.1)	60.6($\pm$10.0)
CVD	88/82	67.9($\pm$10.3)	163.1($\pm$8.8)	64.5($\pm$11.9)

II. MATERIALS AND PRELIMINARIES

A. SUBJECTS

For a more complete comparison, a total of 340 subjects studied in this study were divided into two groups: one is the healthy college students group without any known disease, the other is the patient group where subjects suffer from known cardiovascular disease (CVD). The protocol of the experiment was designed according to the Declaration of Helsinki and approved by the Ethic Committee (University of Zhengzhou). Participants provided their written informed consent to participate in the study. Physical characteristics of healthy and CVD groups are listed in Table 1. It should be noted, rather than distinguishing between healthy or patients, our study aims to investigate the decomposition performance of the noise-assisted EMD-based algorithms in computational pulse analysis under different conditions, unlike most existing studies of pulse diagnosis, healthy and CVD groups are not within the same age range,

B. EXPERIMENTS

As illustrated in Fig. 1, a pressure snesor–ZM-III pulse appratus made by Shanghai University of TCM are used to acquire wrist pulse signals. This apparatus consists of a wearable wrist band, a force sensor, an cuff and air tubes. According to TCM theory, CVD is related to the Chun position of the left hand. Therefore, wrist pulse signals are captured at the Chun position of the left hand. During collection, each subject is asked to sit in the most comfortable posture and relax for more than 10 minutes. Then, professional technicians palm the Chun position and attach the pulse sensor to subject's arm in order to maintain a constant posture and contact force on the radial artery. The pressure of the pulse sensor on the radial artery is progressively gradually increased until finding the appropriate pulse pressure. Finally, each subject is collected for 10 seconds at a sampling rate of 200 Hz, resulting in a pulse signal with 2000 samples.
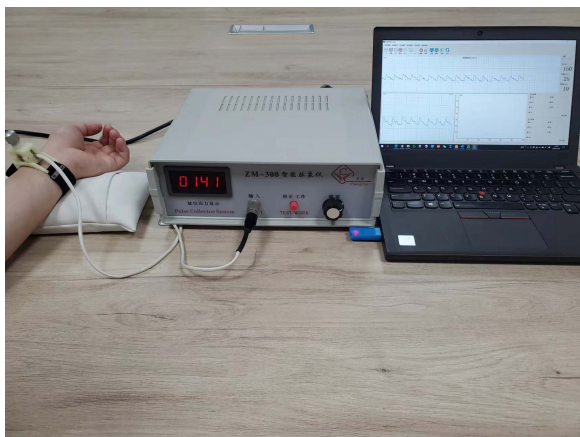

FIGURE 1. Wrist pulse signal acquisition.

C. DATA PREP-PROCESS

As a weak physiological signal, wrist pulse can be easily contaminated by various kinds of interference, including power frequency disturbances, amplitude oscillation caused breathing, muscle contraction and limb vibration [6], [33]. Previous studies have shown that the wrist pulse signal is usually located at low frequencies. 99% of the spectrum energy of the normal signal is concentrated in 0–20 Hz whereas the frequency range of pulse signal under abnormal condition is higher but still not over 40 Hz [7]. Moreover, information below 1 Hz can also be discarded, due to some uncontrollable movements of the subject's arm. For the preprocessing, we follow the denoising and baseline drift correction methods in [33]. Specifically, we first filter out the baseline drift and the 50 Hz-frequency interference through a zero-phase shift bandpass filter with a bandwidth of 1 Hz to 40 Hz, and then remove the baseline wander by wavelet-based cascaded adaptive filter [34]. After pre-processing, some pulse signals could be further excluded by visual inspection due to technical artifact.

Two raw samples and their preprocessed waveforms of a typical healthy and patient subject are shown in Fig (2). As illustrated, the wrist pulse signals in healthy conditions are observed to have regular and smooth morphologies, whereas in abnormal health conditions the pulse signals become irregular, especially in the falling segment of the pulse. In practice, the quantification of these irregularities can be helpful in correlating with abnormal health conditions.

III. METHODS

In this part, we will briefly review the EMD algorithm as well as the improved noise-assisted versions of EMD used in the study: EEMD, NA-MEMD and MEMD. We recommend readers to see corresponding literatures and references for the details.

Algorithm 1 Algorithm of EMD

1: Indentify all the locations of local extrema (both maxima and minima) of the input signal $x(t)$.
2: Interpolate between all the minima (cf. maxima) to construct the lower (cf. upper) envelope $e_{min}(t)$ (cf. $e_{max}(t)$).

3: Compute the local mean of the envelopes $c(t) = (e_{min}(t) + e_{max}(t))/2$ and subtract it from the signal to get the "modulated oscillation" $d(t) = x(t) - c(t)$.
4: If $d(t)$ satisfies the stopping criterion condition, let $IMF_m = d(t)$ else set $x(t) = d(t)$ and go to Step 1.
5: Subtract the derived IMF from the variable $x(t)$ so that $x(t) := x(t) - IMF_m$ and repeat the above described process.
6: Stop the sifting process when the residual are monotonic–the trend $r(t)$ and no longer IMF can be extracted.

A. EMD

A core innovative in vanilla EMD algorithm is introducing the concept of so-called IMF function, which lend themselves to conveying physically meaningful information with classical
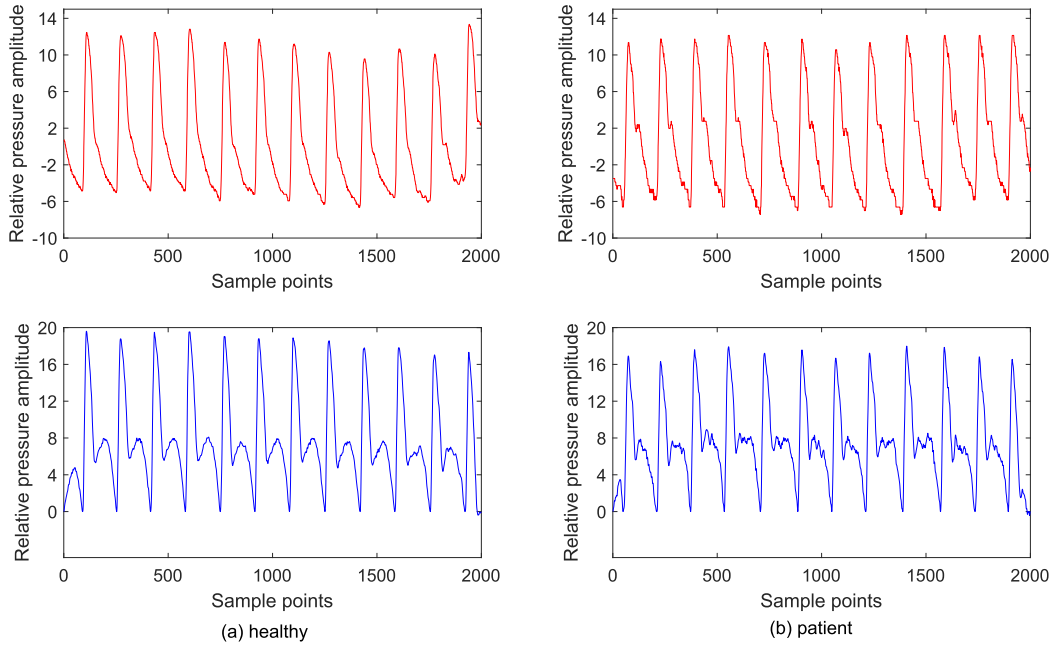
FIGURE 2. Pulse waveform and its filtered results after pre-processing from the left wrist of two typical healthy (a) and patient (b) acquired through the pressure sensor. The top of each subgraph shows the original model and the bottom shows the processed waveform. Note that the wrist pulse signals in healthy conditions are observed to be more regular than that of abnormal health conditions.

Hilbert transform. Specifically, the procedure used to extract an IMF from a signal can be described in Algorithms (1).

B. EEMD AND MEMD

EEMD is the first noise-assisted method to enhance sifting [29], which is based on investigations of the statistical properties of EMD-based decomposition of white gaussian noise (WGN) [35]. Briefly, the EEMD defines the true IMF components as the mean of an ensemble of trials, each is consist of the signal with added white noise of finite amplitude. As a latest variation of EEMD, Median EMD method was proposed by Lang *et al.* [32], in which the mean operator is replaced by the median operator during the ensemble process. With toy numerical signal and industrial case study, it demonstrated that the performance of median EMD is better than ensemble EMD. Together, the specific process steps of EEMD (MEMD) are formulated as follows in Algorithms (2).

Algorithm 2 Algorithm of EEMD and MEMD

1: Generate the ensemble of noise-added original signals: $s_m(t) = x(t) + w_m(t)$ for $m = 1, \cdots, M$, where $w_m(t) \sim \mathcal{N}(0, \sigma^2)$.

2: Decompose each item of the ensemble $s_m(t)$ into M_m IMFs using standard EMD, yielding the set $\{c_k^m(t)\}_{k=1}^{M_m}$.

3: For EEMD, computing the mean under the same-index IMFs $c_k^m(t)$ across the ensemble, that is $\bar{c}_m(t) = (1/M) \sum_{k=1}^{M} c_k^m(t)$. For MEMD, using the median operato, that is $\bar{c}_m(t) = median\{c_m^1(t), c_m^2(t), \cdots, c_m^M(t)\}$.

C. NA-MEMD

The key idea of NA-MEMD is to create an ''composite'' space instead of directly adding noise to n-channel multivariate data. This space is a $(n+l)$-dimensional and consist of two parts, one is n-dimensional signal subspace, the other is an adjacent subspace of l-independent WGN realizations. With the advantage of the filterbank property of multivariate EMD for WGN, the subsequent decomposition produces $(n + l)$-variate coherent IMFs By discarding the l channels pertaining to the noise subspace, the n-variate IMFs can be extracted from the $(n + l)$-variate IMFs, which are corresponding to the original signal.[1] Because of disjoint nature of the signal and noise subspaces, residual noise and mode mixing can also be reduced in the NA-MEMD. The corresponding specific process of NA-MEMD is as follows in Algorithms (3).

IV. EVALUATION METRICS

Due to the empirical definition of the EMD, there is still a lack of general or strict objective metrics for decomposed set evaluation. Several quantitative metrics are available based on ideal conditions IMFs are expected to possess. With a consideration of similar studies on objective assessment [36], [37], evaluation metrics used in this study are tabulated in Table (2).

---

[1]In our case for univariate signal, only those IMFs from the first channel are retrieved.

Algorithm 3 Algorithm of NA-MEMD

1: Creates $l(\geq 1)$-channel white Gaussian noise time series with the same length as that of n-channel input $x(t)$ and add the generated noise to produce a new $p\ (= l + n)$-dimensional signal $y(t)$.

2: Create a suitable set of direction vector $\{X^{\theta_k}\}_{k=1}^K$ on the $(p-1)$ sphere with the aid of a sampling scheme based on the Hammersley sequence and Calculate the projections $\{q_{\theta_v}(t)\}_{v=1}^V$ of the new signal $y(t)$ along these direction vectors.

3: Find the time instant $\{t_{\theta_v}^i\}_{v=1}^V$ corresponding to the maximum value of the projected signal set $\{q_{\theta_v}(t)\}_{v=1}^V$ and interpolate $[t_{\theta_v}^i, y(t_{\theta_v}^i)]$ to get the multivariate envelope curves $\{e_{\theta_v}(t)\}_{v=1}^V$.

4: Calculate mean of the envelopes by $c(t) = \frac{1}{V}\sum_{v=1}^V e_{\theta_v}(t)$.

5: Extract the "detail" $d(t) = y(t) - c(t)$. If $d(t)$ satisfies the stop criteria, apply the above procedure to $y(t) - c(t)$, else repeat for $d(t)$.

6: Choose only the extracted IMFs corresponding to the input signal $x(t)$ from the resulting $(n + l)$-variate IMFs, and discard the IMFs associated with the noise channels.

TABLE 2. Evaluation metrics of EMD-based decomposition.

Metric	Description
NI	Decomposition number of IMF components
f_c	Central frequency of IMF components
OI	Overall extent of orthogonality among IMF components
MM	Overlap of frequency information among successive IMF components

A. NUMBER AND CENTRAL FREQUENCY OF IMFs

The first primary goal of EMD analysis is to identify physically meaningful intrinsic oscillatory modes within the raw signal and extract them as IMFs [36]. As discussed in Pegram *et al.* [38], the smaller number of decomposed IMFs it has, the more likely any meaningful signal it can identify. Moreover, the frequency of the pulse signal is mostly within $1 - 20$Hz, no more than 40Hz. To find those out-of-range components (< 1Hz or > 40Hz), the central frequency of IMF components can be calculated from the power spectral density. Therefore, number and central frequency of IMFs are the most intuitive metrics for decomposition quality.

B. ORTHOGONALITY

Total index of orthogonality characterizes the overall orthogonality among IMFs. Original definition to examine orthogonality [21] is not strictly reversible. To avoid any ambiguity, we employ modified total index of orthogonality, proposed in [36]

$$\mathrm{OI} = \frac{\sum_{m=1}^{M}\sum_{j=1}^{j<i}\left|\sum_{t=1}^{N}(\mathrm{IMF}_i(t) \times \mathrm{IMF}_j(t))\right|}{\sum_{t=1}^{N}(x(t) - r(t))^2} \tag{1}$$

where N is the record length of the original signal $x(t)$, M is the number of IMFs, t is the time step, and i, j the index of IMFs. Note that the EMD residual $r(t)$ is intentionally removed from the original signal to prevent any trend in it. The advantage of the OI indicator is that destructive impact of opposite vector is absolutely suppressed by taking the absolute value of IMF vector product. OI approximating 0 indicates a well decomposition orthogonality.

C. MODE MIXING

The mode mixing effect describes the frequency overlap among the decomposed IMFs within one pulse signal, which would reflect whether a single IMF contains multiple scales and/or a single scale resides in multiple IMFs [37]. Mode-mixing $\mathrm{MM}_{i,j}$ between ith IMF ($\mathrm{IMF}_i(t)$) and jth IMF ($\mathrm{IMF}_j(t)$) can be expressed by the following frequency formulation [37]

$$\Delta f = \max([f_{c2i}, f_{c8i}] \cap [f_{c2j}, f_{c8j}]) \\ - \min([f_{c2i}, f_{c8i}] \cap [f_{c2j}, f_{c8j}]) \tag{2}$$

$$\mathrm{MM}_{i,j} = \frac{\Delta f}{\min\{|f_{c2i} - f_{c8i}|, |f_{c2j} - f_{c8j}|\}} \times 100\% \tag{3}$$

where f_{c2i} and f_{c8i} are central frequencies where 20% and 80% of the energy of ith IMF ($\mathrm{IMF}_i(t)$) are reached, respectively.

V. EXPERIMENTAL RESULTS

In this section, the performance of EMD algorithms mentioned in Section III are evaluated by using real pulse signals and metrics described in Section IV. Followed by parameter settings, the performance of the vanilla EMD is first evaluated as a baseline for contrast purpose. Thereafter, for each noise-assisted EMD, five runs with pre-defined noise characteristics are performed to get statistically reliable performance results. Since the degree of non-linearity is reported to be different among heart disease group and healthy group in [9], for better comparison, the results of healthy and patient groups are shown individually.

A. PARAMETER SETTINGS

Although there is no general principles for selecting EMD parameters, some common instructions and rule of thumb can be followed as described in [29], [37]. All possible combinations of the following parameters are listed as follows.

- **EEMD/MEMD**: number of iterations: 50, 100, 250, 500, 1000.
- **NA-MEMD**: number of extra channels: 2, 3, 4; number of direction vectors: 8, 16, 32, 64.

For all noise-assisted EMDs, the sigma of noise is set to $\{0.1, 0.15, 0.2, 0.25, 0.3\}$. Other parameters such as sifting stopping criteria, interpolation functions and boundary conditions use default values. All the programs are conducted in MATLAB. EMD and EEMD are from commonly-used online available code [39], while the code provided in [40] is used for NA-MEMED. We program MEMD based on EEMD since it differs from EEMD only by using the median operator instead of mean opeartor.
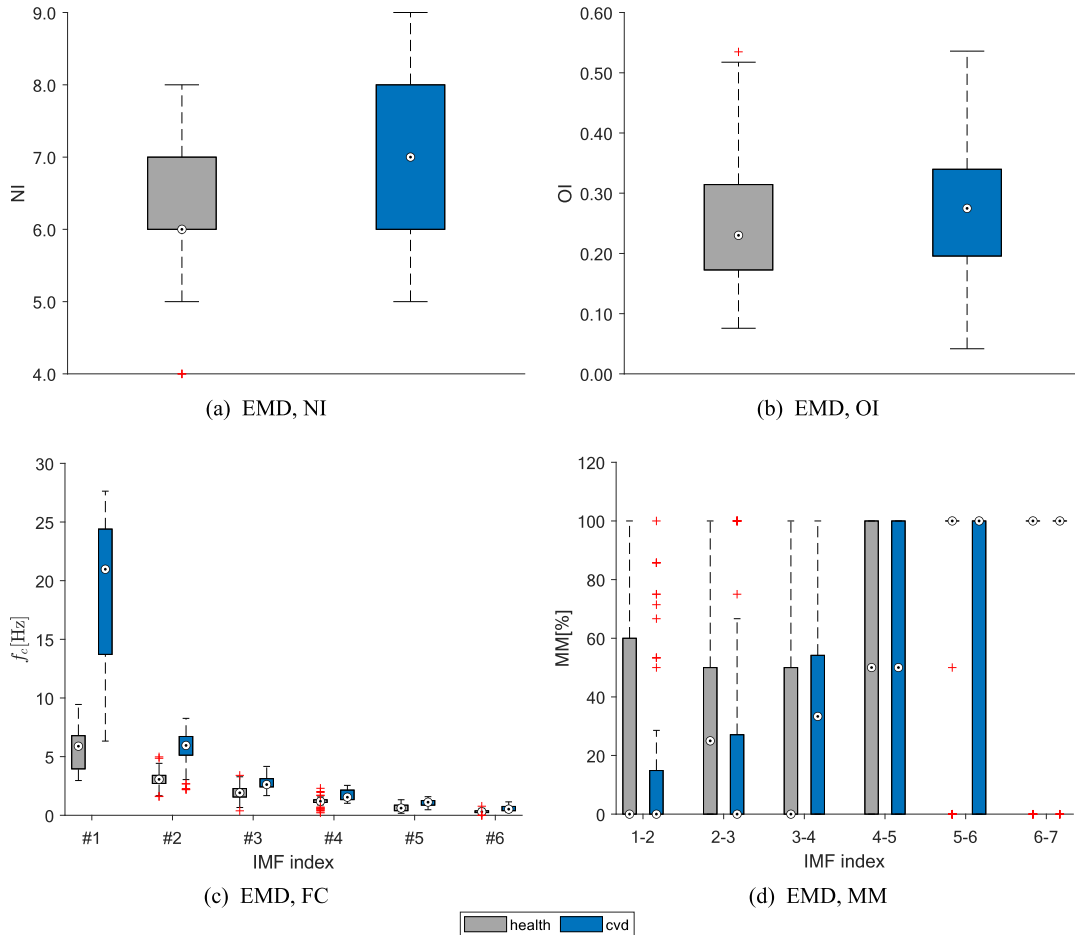
(a) EMD, NI

(b) EMD, OI

(c) EMD, FC

(d) EMD, MM

FIGURE 3. Evaluation metrics with the vanilla EMD.

B. EVALUATION BENCHMARK

Evaluation metrics of the vanilla EMD are served as performance baseline, which are shown separately with NI and OI and f_c and MM in Figure 3 for better presentation.

Figure 3(a) shows that EMD decomposes pulse signals into slightly more components in healthy groups (6 ∼ 7) than that in CVD groups (7 ∼ 8). The reason for this is that as shown in Fig. 2, there are more glitches in pulse signals of CVD groups, which behave more disordered than that of healthy groups. As demonstrated in Figure 3(b), vanilla EMD can not guarantee the orthogonality of each component in reality, with an average index of 0.25 for healthy groups and 0.28 for CVD groups.

As can be seen in Figure 3(c), the overall f_c of healthy groups is below 10 Hz with the highest value of 6 Hz, whereas it is up to 20 Hz for CVD groups. f_c starts below 1 Hz from the 5th component in both groups, indicating that first 4 IMF components are most physiologically relevant. As a result, there is a high chance that the rest of components contain no relevant information of human body, which can be attributed to remaining artifacts due to respiratory movement or vasomotion. In terms of number of IMFs, EMD typically produces 1 ∼ 2 components outside the frequency range

of interset, which should be avoided in subsequent signal analysis.

Figure 3(d) shows that for all groups, MM is almost more than 30% with a very large variance. It is observed that MM of individuals is unpredictable and can be 0 or quite large. This phenomenon demonstrates the instability of vanilla EMD.

From evaluation results in Figure 3, the issue of vanilla EMD can be found, that is it can not guarante orthogonality, which leads to a large mode confusion and some redundancy. This is exactly the deficiency that following noise-assist ed EMDs are intended to improve.

## C. PERFORMANCE COMPARISION

1) NUMBER OF IMFs

Number of IMFs decomposed with noise-assisted EMDs is summarized in Figure 4. It is clear that regardless of noise-assisted EMDs used, more IMF componens are decomposed than that using vanilla EMD.

More specifically, EEMD produces the most IMFs (9 ∼ 10) while NA-MEMD provides the fewest IMFs (7 ∼ 8), and MEMD is in the middle (8 ∼ 9). Although number of IMFs difference among the three EMDs (about 2 ∼ 3) is not significant, NA-MEMD outperforms the
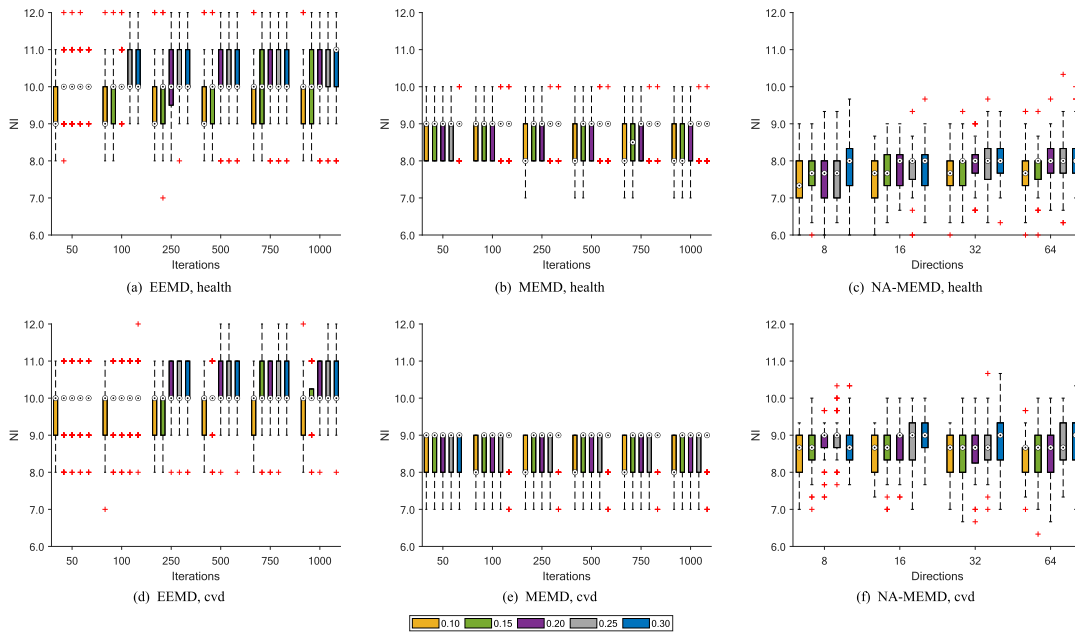
FIGURE 4. Number of IMFs with EEMD, MEMD and NA-MEMD for health and cvd groups. The NI values of NA-MEMD are averaged on extra channels.
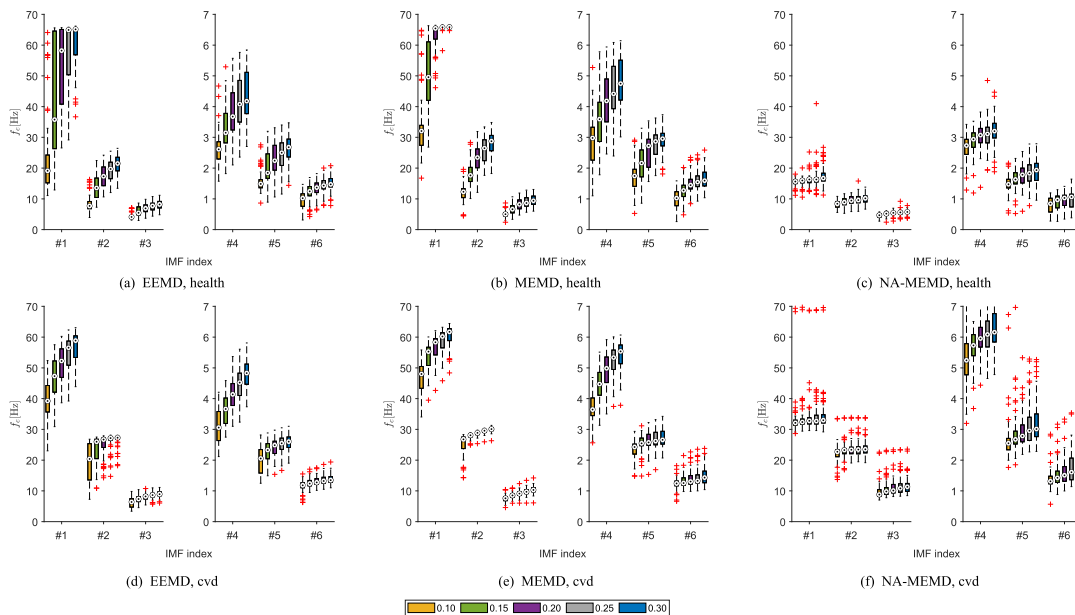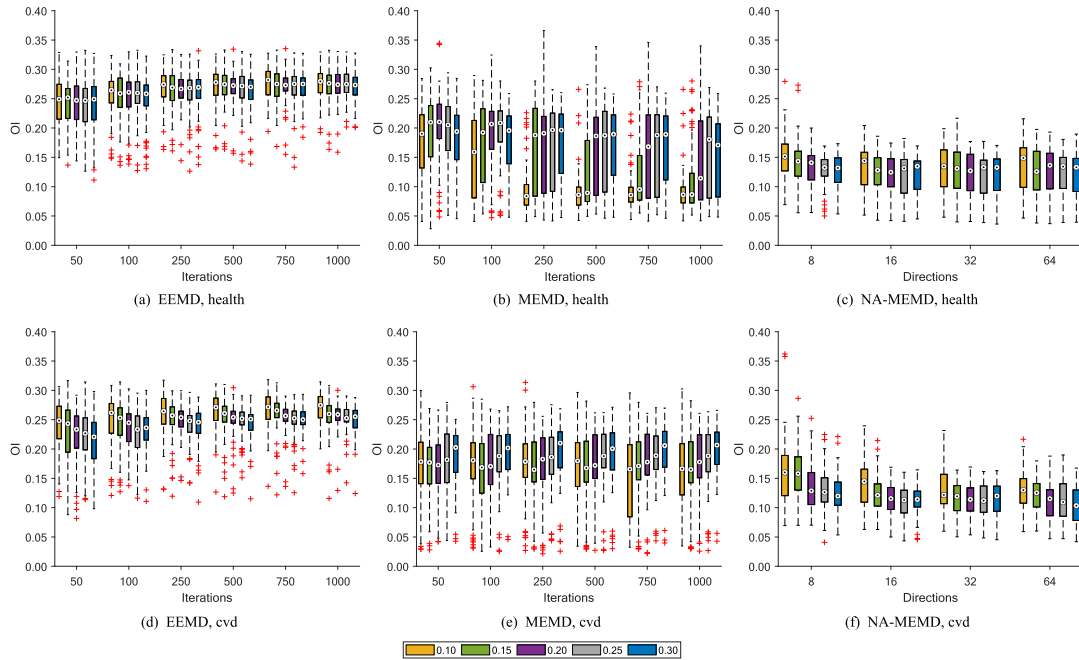

FIGURE 5. Central frequency of IMFs with EEMD, MEMD and NA-MEMD for health and cvd groups. The f_c values are averaged on iterations for EEMD and MEMD, and on extra channels and directions for NA-MEMD.

others and is most competitive to vanilla EMD. For different noise and iterations, NI of MEMD remains basically unchanged, which is more stable than EEMD, especially when the sigma of noise is less than 0.15 and number of iterations is lower than 100. Similarly, NA-MEMD produces almost the same IMF components irrespective of directions. Besides, each noise-assisted EMD has a lower variance for NI than vanilla EMD, indicating that the noise-assisted method indeed reduce the instability to a certain extent.

2) CENTRAL FREQUENCY OF IMFs

For clarity, only the first 6 central frequency of IMF components is depicted in Figure 5. It is surprised that for EEMD and MEMD, f_c of the first IMF component is quite large and beyond the effective frequency range. However, it can be seen that the variance is also relatively large. It implies that the first component is not always redundant, which should be carefully considered in practice. Therefore, the effective pulse signal is mainly concentrated in IMFs $2 \sim 5$. Considering NI

FIGURE 6. Orthogonality index with EEMD, MEMD and NA-MEMD for health and cvd groups. The OI values of NA-MEMD are averaged on extra channels.
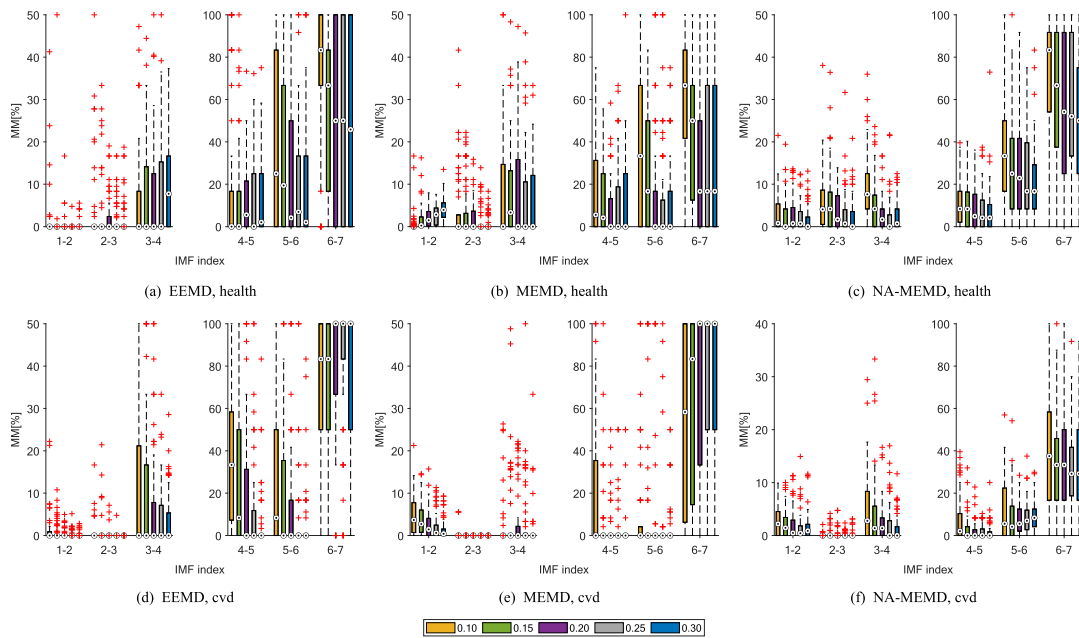
FIGURE 7. Mode mixing with EEMD, MEMD and NA-MEMD for health and cvd groups. The MM values are averaged on iterations for EEMD and MEMD, and on extra channels and directions for NA-MEMD.

in vanilla EMD shown in the Figure 3(a), EEMD produces $5 \sim 6$ redundancies and MEMD produces $4 \sim 5$ redundancies. For noise-assisted EMDs, f_c of IMFs $2 \sim 5$ is larger than the counterpart in vanilla EMD and increases with the added noise amplitude increases. When the assisted noise has the smallest amplitude (0.1), EEMD is closest to vanilla EMD among the three with respect to f_c of valid IMFs. This

phenomenon demonstrates that introducing noise can bring unnecessary information, especially as the central frequency of different numbers of components fluctuates greatly as the noise increases.

It appears that f_c of the first 5 IMFs using NA-MEMD are all within the valid frequency range (see Figure 5(c) and Figure 5(f)). Although f_c of IMF 1 is much lower than

that of EEMD and MEMD, it is actually considered to be redundant compared with vanilla EMD, resulting in only $2 \sim 3$ redundancies introduced. In this aspect, NA-MEMD algorithm may be a better choice for pulse signal processing, which has not been applied in the existing literature. Since the center frequency of each component has little fluctuation and the variance is small under different noise conditions, NA-MEMD algorithm has better stability than EEMD and MEMD.

3) ORTHOGONALITY INDEX
The total orthogonality indexes of the decomposed IMF components is shown Figure 6. It can be observed that the orthogonality of EEMD does not differ significantly from vanilla EMD, where CVD groups is slightly better than healthy groups. It can be argued that there is no benefit in orthogonality from assisted noise when using EEMD. However, it is improved dramatically by MEMD with the index dropping below 0.2, which confirms the fact that the median operator is superior to the mean operator. The best orthogonality achieved is NA-MEMD, whose index is lower than 0.15. In addition, the noise amplitude has little effect on the orthogonality index.

4) MODE MIXING
The mode mixing along all pulse signals for these noise-assited EMD methods was calculated and illustrated in Figure 7. It should be emphasized here that only the first six components are taken into consideration.

As expected, the mode mixing can be considerably reduced by introducing noise for both healthy and CVD groups. Compared with the mode mixing with vanilla EMD, which is generally higher than 30% (Figure 3(d)), it is less than 20% with noise-assisted EMDs and the variance is also smaller (Figure 7(c) and Figure 7(f)). Again, it also can be seen that NA-MEMD performs the best mode mixing reduction among three EMDs.

VI. DISCUSSION
In the present study, three representative noise-assisted EMD candidates (EEMD, MEMD and NA-MEMD) have been thoroughly investigated with real wrist pulse signals from health and patient groups. Before our works, seldom have applied MEMD and NA-MEMD to wrist pulse signals. Based on evaluation results with four objective metrics, some valuable observations should deserve more attention in practice.

Firstly, performance of three noise-assisted EMDs is better than vanilla EMD in terms of those objective indexes except for number of IMFs. Overall, comparative results manifest that NA-MEMD should be more suitable for pulse signals rather than the recently proposed MEMD. EEMD and MEMD require the noise well chosen while NA-MEMD is more relatively robust to noise. Moreover, EEMD and MEMD are more likely to be influenced by the chosen noise, while NA-MEMD is robust to this. Although results shows effectiveness of NA-MEMD, which is still far from the ideal

condition for complete orthogonality, there still has much room to improve the performance further. On the other hand, the performance of different proposed algorithms is usually only demonstrated by synthesis signals or with visual inspection for signals in other fields. Our experimental results on wrist pulse signals suggests that it will be more convincing for other physiological signal analysis by using more real-world signals and objective indicators in practice.

Secondly, introducing noise into EMD can indeed improve performance on many metrics, but one of serious side effects is introducing additional redundant components. To the best of our knowledge, in TCM community, a lot of effort have been made to the improve the performance by assisted noise, but seldom mentioned the redundancy caused by those assisted noise. Physiologically irrelevant redundancy mainly comes from intrinsic activities such as residual respiration or vasomotion components after removing interference for vanilla EMD, and from residual noise for noise-assisted EMDs. In terms of redundancy, vanilla EMD produces at most 2 redundancies but it is up to 6 for noise-assisted EMDs. In this aspect, the closest to vanilla EMD is NA-MEMD with a redundancy of 3, because the noise and the signal are combined in a channel way rather than being directly aggregated. Actually proponents of NA-MEMD has pointed out the fact that adding noise directly to the data could cause residual noise to remain in IMFs [31]. Nowadays, EMD algorithms are mostly used as signal decomposition methods for feature extraction, and thus careful exclusion of redundant components before extraction is expected to further improve classification accuracy.

Finally, although this present study has elaborately presented the comparative study of typical EMDs for pulse signals, there are still some issues to make clear or worthy of further in-depth research.

- In addition to the parameters specified in Section V-A, several factors of the EMD algorithm itself, such as interpolation and end effects, also contribute to the final signal decomposition. Specialized fine-tuning of associated parameters could be very useful. However, it should be noted that our main goal of this paper is to evaluate and compare the performance under the same conditions as fairly as possible. Unless there is a mathematical foundation of the EMD, it is impossible to construct some definitive metrics that capture all the key features. Evaluation measures proposed in our paper could be considered as an assistance for researchers in TCM community when choosing EMD algorithms.
- Since the EMD algorithms study in this paper are representative, evaluating on some enhanced versions of EEMD (complementary EMD [41], complete EMD [42] and improved complete EMD [43]) with their own advantages is deserved to be a future research direction. In addition, objective metrics can also be further extended by considering different modal decomposition algorithms [44], such as variational mode decomposition [45], [46] and nonlinear mode decomposition [47].

VII. CONCLUSION

EMD and its improved noise-assisted versions have been proved to be more suitable than traditional methods for the analysis of non-linear and non-stationary signals, but is less explored in pulse signal analysis. With real recorded pulse signals from healthy and patient groups, a systematically comparative study on three noise-assisted EMD algorithms in terms of multiple objective quantitative metrics are examined in this paper. Experimental results show that NA-MEMD rather very recently MEMD, is consistently superior to the others and potentially most efficient for computational pulse analysis/diagnosis.

However, it needs to be noted that performance benefits gained by assisted noise is at the expense of introducing additional redundancy. We argue that this is of great practical sense and supposed to attract more attention, since redundancy elimination is expected to further enhance the performance of intelligent pulse diagnosis. We believe the study of this paper could provide new insights and best practices for the successful use in computational analysis or diagnosis for wrist pulse signals as well as other physiological signals that are methodologically similar.

ACKNOWLEDGMENT

REFERENCES

[1] Z. Fei, *Contemporary Sphygmology in Traditional Chinese Medicine*. Beijing, China: People's Medical Publishing House, 2003.

[2] C. Zhao, G.-Z. Li, C. Wang, and J. Niu, "Advances in patient classification for traditional Chinese medicine: A machine learning perspective," *Evidence-Based Complementary Alternative Med.*, vol. 2015, pp. 1–18, Apr. 2015.

[3] Z. Jiang, D. Zhang, and G. Lu, "A robust wrist pulse acquisition system based on multisensor collaboration and signal quality assessment," *IEEE Trans. Instrum. Meas.*, vol. 68, no. 12, pp. 4807–4816, Dec. 2019.

[4] Q. Zhang, J. Zhou, and B. Zhang, "Graph based multichannel feature fusion for wrist pulse diagnosis," *IEEE J. Biomed. Health Informat.*, vol. 25, no. 10, pp. 3732–3743, Oct. 2021.

[5] Q. Zhang, J. Zhou, and B. Zhang, "Computational traditional Chinese medicine diagnosis: A literature survey," *Comput. Biol. Med.*, vol. 133, Jun. 2021, Art. no. 104358.

[6] C. Guo, Z. Jiang, H. He, Y. Liao, and D. Zhang, "Wrist pulse signal acquisition and analysis for disease diagnosis: A review," *Comput. Biol. Med.*, vol. 143, Apr. 2022, Art. no. 105312.

[7] D. Zhang, W. Zuo, and P. Wang, *Computational Pulse Signal Analysis*. Singapore: Springer, 2018.

[8] D. T. Kaplan, "Nonlinearity and nonstationarity: The use of surrogate data in interpreting fluctuations," in *Frontiers of Blood Pressure and Heart Rate Analysis*. Amsterdam, The Netherlands: IOS Press, 1997, pp. 15–28.

[9] J. Yan, Y. Wang, C. Xia, F. Li, and R. Guo, "Detecting nonlinearity in wrist pulse using delay vector variance method," in *Advances in Cognitive Neurodynamics ICCN 2007*. Berlin, Germany: Springer, 2008, pp. 867–871.

[10] C. T. Lee and L. Y. Wei, "Spectrum analysis of human pulse," *IEEE Trans. Biomed. Eng.*, vol. BE-30, no. 6, pp. 348–352, Jun. 1983.

[11] L. Y. Wei and P. Chow, "Frequency distribution of human pulse spectra," *IEEE Trans. Biomed. Eng.*, vol. BE-32, no. 3, pp. 245–246, Mar. 1985.

[12] L. Xu, K. Wang, and D. Zhang, "Modern researches on pulse waveform of TCPD," in *Proc. IEEE Int. Conf. Commun., Circuits Syst. West Sino Expo.*, vol. 2, Jun. 2002, pp. 1073–1077.

[13] L. Xu, M. Q.-H. Meng, C. Shi, K. Wang, and N. Li, "Quantitative analyses of pulse images in traditional Chinese medicine," *Med. Acupuncture*, vol. 20, no. 3, pp. 175–189, Sep. 2008.

[14] D. Zhou and K. B. Cai, "The pulse signals pattern identification method based on short-time Fourier transform," *J. Chongqing Univ. Sci. Technol.*, vol. 3, pp. 49–52, Sep. 2007.

[15] Z. Jiang, C. Guo, J. Zang, G. Lu, and D. Zhang, "Features fusion of multichannel wrist pulse signal based on KL-MGDCCA and decision level combination," *Biomed. Signal Process. Control*, vol. 57, Mar. 2020, Art. no. 101751.

[16] D. Jia, N. Li, S. Liu, and S. Li, "Decision level fusion for pulse signal classification using multiple features," in *Proc. 3rd Int. Conf. Biomed. Eng. Informat.*, vol. 2, Oct. 2010, pp. 843–847.

[17] D. Y. Zhang, W. M. Zuo, D. Zhang, H. Z. Zhang, and N. M. Li, "Wrist blood flow signal-based computerized pulse diagnosis using spatial and spectrum features," *J. Biomed. Sci. Eng.*, vol. 3, no. 4, p. 361, 2010.

[18] L. Liu, W. Zuo, D. Zhang, N. Li, and H. Zhang, "Combination of heterogeneous features for wrist pulse blood flow signal diagnosis via multiple kernel learning," *IEEE Trans. Inf. Technol. Biomed.*, vol. 16, no. 4, pp. 598–606, Jul. 2012.

[19] D. P. Mandic, N. U. Rehman, Z. Wu, and N. E. Huang, "Empirical mode decomposition-based time-frequency analysis of multivariate signals: The power of adaptive data analysis," *IEEE Signal Process. Mag.*, vol. 30, no. 6, pp. 74–86, Nov. 2013.

[20] B. Boashash, *Time-Frequency Signal Analysis and Processing: A Comprehensive Reference*. New York, NY, USA: Academic, 2015.

[21] N. E. Huang, S. R. Long, M. C. Wu, H. H. Shih, Q. Zheng, N. C. Yen, C. C. Tung, H. H. Liu, and Z. Shen, "The empirical mode decomposition and the Hilbert spectrum for nonlinear and non-stationary time series analysis," *Proc. Roy. Soc. London A, Math., Phys. Eng. Sci.*, vol. 454, no. 1971, pp. 903–995, 1998.

[22] C. M. Sweeney-Reed, S. J. Nasuto, M. F. Vieira, and A. O. Andrade, "Empirical mode decomposition and its extensions applied to EEG analysis: A review," *Adv. Data Sci. Adapt. Anal.*, vol. 10, no. 2, Apr. 2018, Art. no. 1840001.

[23] M.-H. Lee, K.-K. Shyu, P.-L. Lee, C.-M. Huang, and Y.-J. Chiu, "Hardware implementation of EMD using DSP and FPGA for online signal processing," *IEEE Trans. Ind. Electron.*, vol. 58, no. 6, pp. 2473–2481, Jun. 2011.

[24] R. Sun, H. Shen, C. Lu, Y. Wang, and F. Li, "Application of the HHT method to the wrist-pulse-signal analysis," *J. Med. Biomech.*, vol. 2, pp. 87–93, Jun. 2006.

[25] H. Xing, R. Xu, and C. Wang, "Pulse signal feature research based on empirical mode decomposition," *Chin. J. Sci. Instrum.*, vol. 30, no. 3, pp. 596–602, 2009.

[26] Y. Li, F. Wang, R. Sun, S. Xue, D. Yao, and H. Shen, "Pulse wave analysis in patients with coronary heart disease based on Hilbert–Huang transformation and time–domain," *Chin. J. Biomed. Eng.*, vol. 22, no. 2, pp. 47–54, 2013.

[27] R. Guo, Y. Wang, H. Yan, J. Yan, F. Yuan, Z. Xu, G. Liu, and W. Xu, "Analysis and recognition of traditional Chinese medicine pulse based on the Hilbert–Huang transform and random forest in patients with coronary heart disease," *Evidence-Based Complementary Alternative Med.*, vol. 2015, pp. 1–8, Jan. 2015.

[28] F.-F. Li, R. Sun, S. Xue, P. Qian, H.-X. Yan, W.-F. Zhang, Z.-M. Sun, H.-K. Zhang, and Y.-Q. Wang, "Pulse signal analysis of patients with coronary heart diseases using Hilbert–Huang transformation and time-domain method," *Chin. J. Integrative Med.*, vol. 21, no. 5, pp. 355–360, May 2015.

[29] Z. Wu and N. E. Huang, "Ensemble empirical mode decomposition: A noise-assisted data analysis method," *Adv. Adapt. Data Anal.*, vol. 1, no. 1, pp. 1–41, 2009.

[30] N. U. Rehman and D. P. Mandic, "Filter bank property of multivariate empirical mode decomposition," *IEEE Trans. Signal Process.*, vol. 59, no. 5, pp. 2421–2426, May 2011.

[31] N. U. Rehman, C. Park, N. E. Huang, and D. P. Mandic, "EMD via MEMD: Multivariate noise-aided computation of standard EMD," *Adv. Adapt. Data Anal.*, vol. 5, no. 2, 2013, Art. no. 1350007.

[32] X. Lang, N. U. Rehman, Y. Zhang, L. Xie, and H. Su, "Median ensemble empirical mode decomposition," *Signal Process.*, vol. 176, Nov. 2020, Art. no. 107686.

[33] D. Wang, D. Zhang, and G. Lu, "A robust signal preprocessing framework for wrist pulse analysis," *Biomed. Signal Process. Control*, vol. 23, pp. 62–75, Jan. 2016.

[34] L. Xu, D. Zhang, and K. Wang, "Wavelet-based cascaded adaptive filter for removing baseline drift in pulse waveforms," *IEEE Trans. Biomed. Eng.*, vol. 52, no. 11, pp. 1973–1975, Nov. 2005.

[35] P. Flandrin, P. Gonçalves, and G. Rilling, "EMD equivalent filter banks, from interpretation to applications," in *Hilbert–Huang Transform and its Applications*. Singapore: World Scientific, 2005, pp. 57–74.

[36] M. C. Peel, T. A. McMahon, and G. G. S. Pegram, "Assessing the performance of rational spline-based empirical mode decomposition using a global annual precipitation dataset," *Proc. Roy. Soc. A, Math., Phys. Eng. Sci.*, vol. 465, no. 2106, pp. 1919–1937, Jun. 2009.

[37] M. Lozano, J. A. Fiz, and R. Jané, "Performance evaluation of the Hilbert–Huang transform for respiratory sound analysis and its application to continuous adventitious sound characterization," *Signal Process.*, vol. 120, pp. 99–116, Mar. 2016.

[38] G. G. S. Pegram, M. C. Peel, and T. A. McMahon, "Empirical mode decomposition using rational splines: An application to rainfall time series," *Proc. Roy. Soc. A, Math., Phys. Eng. Sci.*, vol. 464, no. 2094, pp. 1483–1501, Jun. 2008.

[39] G. Rilling, P. Flandrin, and P. Goncalves, "On empirical mode decomposition and its algorithms," in *Proc. IEEE Workshop Nonlinear Signal Image Process. (EURASIP)*, vol. 3, Jun. 2003, pp. 8–11.

[40] D. Mandic. (2017). *Diy Corpora: The WWW and the Translator*. [Online]. Available: https://www.commsp.ee.ic.ac.uk/~mandic/research/emd.htm

[41] J. R. Yeh, J. S. Shieh, and N. E. Huang, "Complementary ensemble empirical mode decomposition: A novel noise enhanced data analysis method," *Adv. Adapt. Data Anal.*, vol. 2, no. 2, pp. 135–156, 2010.

[42] M. E. Torres, M. A. Colominas, G. Schlotthauer, and P. Flandrin, "A complete ensemble empirical mode decomposition with adaptive noise," in *Proc. IEEE Int. Conf. Acoust., Speech Signal Process. (ICASSP)*, May 2011, pp. 4144–4147.

[43] M. A. Colominas, G. Schlotthauer, and M. E. Torres, "Improved complete ensemble EMD: A suitable tool for biomedical signal processing," *Biomed. Signal Process. Control*, vol. 14, pp. 19–29, Nov. 2014.

[44] H.-T. Wu, "Current state of nonlinear-type time–frequency analysis and applications to high-frequency biomedical signals," *Current Opinion Syst. Biol.*, vol. 23, pp. 8–21, Oct. 2020.

[45] K. Dragomiretskiy and D. Zosso, "Variational mode decomposition," *IEEE Trans. Signal Process.*, vol. 62, no. 3, pp. 531–544, Feb. 2014.

[46] Q. Ni, J. C. Ji, K. Feng, and B. Halkon, "A fault information-guided variational mode decomposition (FIVMD) method for rolling element bearings diagnosis," *Mech. Syst. Signal Process.*, vol. 164, Feb. 2022, Art. no. 108216.

[47] D. Iatsenko, P. V. E. McClintock, and A. Stefanovska, "Nonlinear mode decomposition: A noise-robust, adaptive decomposition method," *Phys. Rev. E, Stat. Phys. Plasmas Fluids Relat. Interdiscip. Top.*, vol. 92, no. 3, Sep. 2015, Art. no. 032916.

YUNZHI TIAN received the B.S. degree from Xi'an Shiyou University, Xi'an, China, in 2020. He is currently a Graduate Student with the School of Electrical Engineering, Zhengzhou University. His main research interests include biomedical signal analysis and data processing.

QIA WANG received the Ph.D. degree from the Academy of Mathematics and Systems Science, Chinese Academy of Sciences, Beijing, China, in 2013. Now, she is an Associate Professor with the Institute of Quantitative and Technological Economics, Chinese Academy of Social Sciences, Beijing. Her research interests include optimization algorithms and data analysis and processing.

XIAOBO MAO served as a Professor with the School of Electrical Engineering, Zhengzhou University. His current research interests include robot vision, intelligent instrument development, and biomedical signal processing.

YUPING ZHAO served as an Associate Researcher with the China Academy of Chinese Medical Sciences. Her current research interests include the development of traditional Chinese medicine equipment and big data analysis.

HUAXING XU received the Ph.D. degree in engineering from the Institute of Acoustics, Chinese Academy of Sciences, in 2017. Since then, he has been a Lecturer with the School of Electrical Engineering, Zhengzhou University. His current research interests include signal analysis and processing (including audio signal, speech signal, and biomedical signal) and pattern recognition.

LUQI HUANG is currently a Doctoral Supervisor and an Academician with the Chinese Academy of Engineering and the President of the China Academy of Chinese Medical Sciences. His current research interests include the molecular pharmacognosy, traditional Chinese medicine, and big data analysis and processing.

● ● ●